

## Receptor-mediated Targeting of Fluorescent Probes in Living Cells\*

(Received for publication, December 10, 1998, and in revised form, January 7, 1999)

Javier Farinas‡ and A. S. Verkman

From the Departments of Medicine and Physiology,  
Cardiovascular Research Institute, University of  
California, San Francisco, California 94143-0521

A strategy was developed to label specified sites in living cells with a wide selection of fluorescent or other probes and applied to study pH regulation in Golgi. cDNA transfection was used to target a single-chain antibody to a specified site such as an organelle lumen. The targeted antibody functioned as a high affinity receptor to trap cell-permeable hapten-fluorophore conjugates. Synthesized conjugates of a hapten (4-ethoxymethylene-2-phenyl-2-oxazolin-5-one, phOx) and fluorescent probes (Bodipy FL, tetramethylrhodamine, fluorescein) were bound with high affinity (~5 nM) and specific localization to the single-chain antibody expressed in the endoplasmic reticulum, Golgi, and plasma membrane of living Chinese hamster ovary cells. Using the pH-sensitive phOx-fluorescein conjugate and ratio imaging microscopy, pH was measured in the lumen of Golgi ( $\text{pH } 6.25 \pm 0.06$ ). Measurements of pH-dependent vacuolar  $\text{H}^+$ /ATPase pump activity and  $\text{H}^+$  leak in Golgi provided direct evidence that resting Golgi pH is determined by balanced leak-pump kinetics rather than the inability of the  $\text{H}^+$ /ATPase to pump against an electrochemical gradient. Like expression of the green fluorescent protein, the receptor-mediated fluorophore targeting approach permits specific intracellular fluorescence labeling. A significant advantage of the new approach is the ability to target chemical probes with custom-designed spectral and indicator properties.

Small-molecule fluorescent probes have been widely used to study protein localization, cytoplasmic ionic content (1), and solute diffusion (2). Probes are available with high intrinsic brightness and excitation and emission peaks from ultraviolet to infrared wavelengths; however, in general these chemical probes cannot be targeted to specific sites in living cells. The green fluorescent protein (GFP)<sup>1</sup> is a genetically targetable

probe that has been used extensively to study gene expression and protein localization in living cells (3, 4). However, GFP fluorescence is limited to blue, cyan, green, and green/yellow variants, which have relatively low intrinsic brightness (4, 5). GFP-based indicators are currently limited to measuring pH (6–8),  $\text{Ca}^{2+}$  (9, 10), and membrane potential (11).

A cell labeling method is reported here that combines the site specificity conferred by genetically encoded targeting sequences with the excellent spectral and indicator properties of small chemical fluorophores. The strategy is to express a high affinity “receptor” at a specified intracellular location to trap a conjugate of a fluorophore linked to a receptor “ligand” (Fig. 1a). We chose a single-chain antibody (sFv) (12) as the receptor and a hapten (phOx) as the ligand. Although many receptor-ligand pairs are possible, the antibody-hapten pair was selected because of the simple ligand-probe chemistry and high affinity interaction without interference from cellular factors. For sFv targeting, cells are transfected with cDNAs encoding sFv in fusion with targeting sequences. Fluorophore-hapten conjugates are added to the extracellular solution at low concentrations, diffuse to sites of sFv expression, and bind to the sFv. Conjugates of different indicator and spectral properties were synthesized (Fig. 1b), including phOx-Bodipy FL (green fluorescent), phOx-fluorescein (green fluorescent, pH-sensitive), and phOx-tetramethylrhodamine (red fluorescent). The flexible linkers were designed to permit stacking of the unbound hapten with its covalently attached fluorophore to form a dark complex and reduce background fluorescence.

The ability to label cellular sites with fluorescent probes with varied spectral and indicator properties was demonstrated, and the phOx-fluorescein conjugate was applied to measure pH in the Golgi lumen. Here we report the first *in vivo* measurement of the regulation of the pump rate of the vacuolar  $\text{H}^+$ /ATPase by Golgi luminal pH to test the thermodynamic model (13) of how the resting pH is set in organelles such as the Golgi.

### EXPERIMENTAL PROCEDURES

**Plasmids and Cell Transfection**—The cDNA encoding the sFv (25-kDa protein) and two c-Myc epitopes was amplified by polymerase chain reaction using the plasmid pHook1 (12) (Invitrogen) as template, with sense primer (5'GGAATTCGCCGAGGTCAAGCTGCAGGAG3') containing an *EcoRI* site (underlined) and antisense primer containing an *XbaI* site (underlined) (5'GCTCTAGACTGGCCACAGCATTCA-GATCTC3'). For ER and Golgi targeting, the cDNA was subcloned at *EcoRI* and *XbaI* sites in expression plasmid pCDNA3.1 containing specific targeting sequences as described in Ref. 6. Plasma membrane targeting was achieved with the pHook1 plasmid (12). CHO cells (ATCC CRL 9618) were transfected with plasmids encoding targeted sFv using LipofectAMINE (Life Technologies, Inc.) as described previously (6).

**Synthesis of Hapten-Fluorophore Conjugates**—A flexible linker was added to phOx (Sigma) by reaction of 50 mg of phOx with 14.3  $\mu\text{l}$  of 1,5-diaminopentane (Aldrich) in 2.5 ml of acetone for 1 h. The disubstituted aminopentane was precipitated by the addition of 2 volumes of 50 mM borate buffer (pH 9.2), leaving the product in solution. A more rigid linker was added to phOx by reaction of *trans*-1,4-diaminocyclohexane (Aldrich) (5.1 mg in 0.5 ml of  $\text{Me}_2\text{SO}$ ) and phOx (10 mg in 0.5 ml of acetone) for 2 h. The disubstituted diaminocyclohexane was precipitated by the addition of an equal volume of water, leaving the product in solution. phOx-Bodipy FL was prepared by reaction of excess Bodipy FL succinimidyl ester (Molecular Probes) with 1 mM phOx-aminopentane in borate buffer for 2 h. The product was obtained as a precipitate. PhOx-tetramethylrhodamine was prepared by reaction of excess tetramethylrhodamine succinimidyl ester (Molecular Probes) with 5 mM phOx-aminocyclohexane in borate buffer for 6 h. The product was obtained as a precipitate. phOx-fluorescein was prepared by reaction of

\* This work was supported by National Institutes of Health Grants DK43840 and DK35124 and National Cystic Fibrosis Foundation Grant R613. We also acknowledge the University of California, San Francisco mass spectrometry facility, which is supported by National Institutes of Health Grant RR01614. The costs of publication of this article were defrayed in part by the payment of page charges. This article must therefore be hereby marked “advertisement” in accordance with 18 U.S.C. Section 1734 solely to indicate this fact.

‡ To whom correspondence should be addressed: Cardiovascular Research Inst., 1246 Health Sciences East Tower, University of California, San Francisco, CA 94143-0521. Tel.: 415-476-8530; Fax: 415-665-3847; E-mail: javier@itsa.ucsf.edu; http://www.ucsf.edu/verklab.

<sup>1</sup> The abbreviations used are: GFP, green fluorescent protein; phOx, 4-ethoxymethylene-2-phenyl-2-oxazolin-5-one; ER, endoplasmic reticulum; CHO, Chinese hamster ovary.

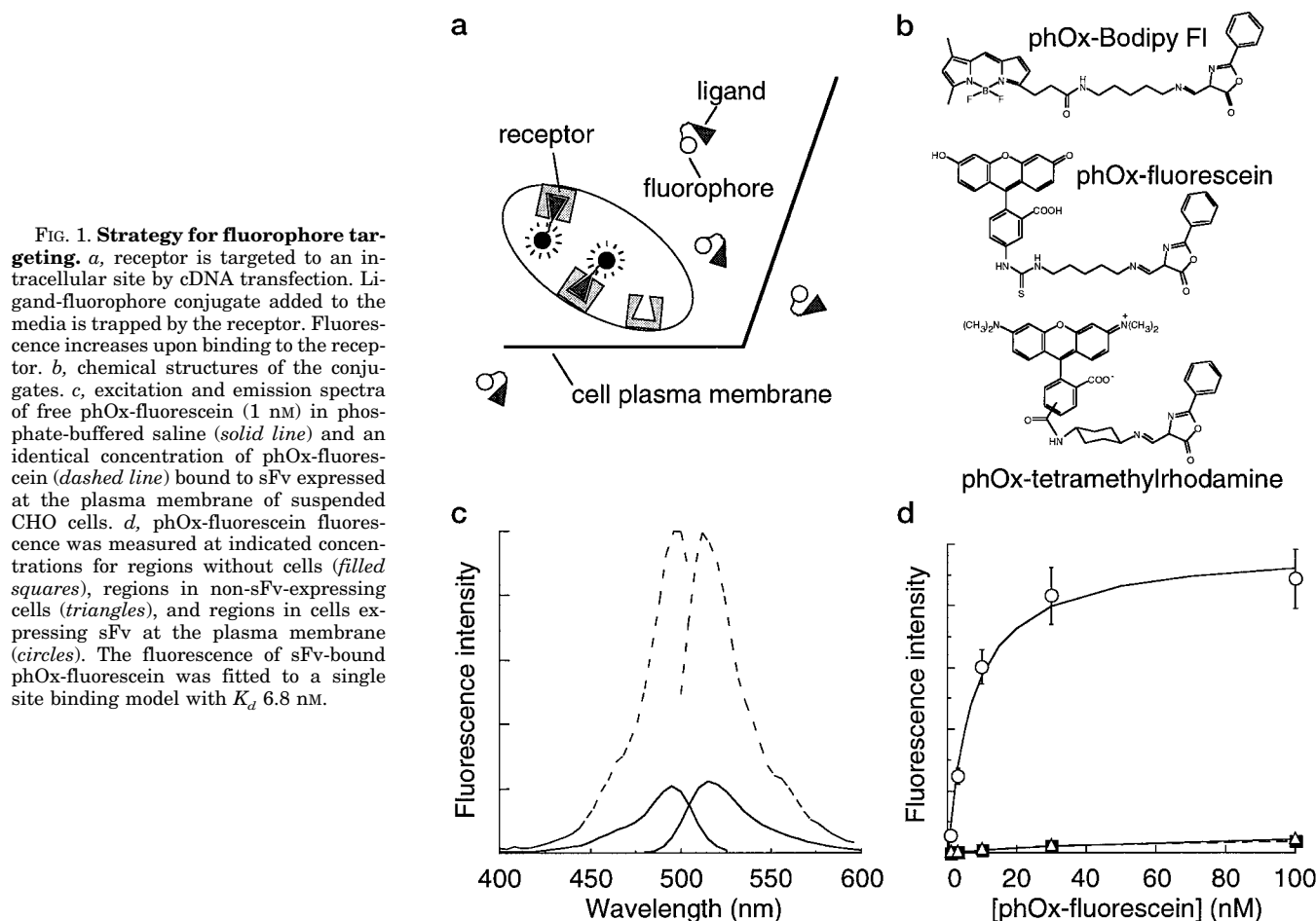


**FIG. 1. Strategy for fluorophore targeting.** *a*, receptor is targeted to an intracellular site by cDNA transfection. Ligand-fluorophore conjugate added to the media is trapped by the receptor. Fluorescence increases upon binding to the receptor. *b*, chemical structures of the conjugates. *c*, excitation and emission spectra of free phOx-fluorescein (1 nM) in phosphate-buffered saline (solid line) and an identical concentration of phOx-fluorescein (dashed line) bound to sFv expressed at the plasma membrane of suspended CHO cells. *d*, phOx-fluorescein fluorescence was measured at indicated concentrations for regions without cells (filled squares), regions in non-sFv-expressing cells (triangles), and regions in cells expressing sFv at the plasma membrane (circles). The fluorescence of sFv-bound phOx-fluorescein was fitted to a single site binding model with  $K_d$  6.8 nM.

equimolar amounts of phOx (0.5 mg in 25  $\mu$ l of acetone) and fluorescein cadaverine (1 mg in 50  $\mu$ l of dimethylformamide; Molecular Probes) for 1 h. Phosphate-buffered saline was added, unreacted phOx was removed by hexane extraction, and the product was extracted with butanol. phOx-ethanolamine was prepared by reaction of 1 mg of phOx with 0.3  $\mu$ l of ethanolamine in 10 ml of ethanol for 1 h. Reactions were conducted at room temperature. Products were judged to be >95% pure by TLC, and structures were confirmed by mass spectrometry.

**Fluorescence Measurements**—Cells were labeled at 2 days after transfection by incubation with low concentrations (<100 nM) of the conjugates. Unless otherwise indicated, cells were observed in the absence of the conjugate in the bathing media. Images were recorded at room temperature on a K2 BIO microscope (Technical Instruments) equipped with a 60 $\times$  PlanApo objective (Nikon, N.A. 1.4), coaxial-confocal attachment, and cooled CCD camera. Dual excitation ratio images of fluorescein were acquired using 440- and 490-nm excitation filters and a 520-nm long pass emission filter. Continuous recordings of the fluorescence time course were obtained on a Nikon Diaphot epifluorescence microscope equipped with a 100 $\times$  PlanApo objective (Nikon, N.A. 1.4), a photomultiplier using a 530-nm bandpass emission filter, and an optical filter changer (model 10-C, Sutter Instrument Co.) containing 440- and 490-nm excitation filters. Cuvette fluorescence measurements were conducted on an SLM 8000c fluorometer (SLM Aminco). Spectra were recorded with 4-nm slit widths; time courses were acquired with 495-nm excitation and 510-nm long pass emission filters.

## RESULTS

For effective targeting, the requirements of the sFv/hapten-fluorophore system include: bright fluorescence of the bound conjugate, high affinity binding of the conjugate to sFv, stability of the conjugate, minimal cellular toxicity, strong cellular expression of functional sFv, and membrane permeability of the conjugate. These requirements were fulfilled for cellular sFv expression (using the Golgi, ER, and plasma membrane vectors) and binding of the conjugates in Fig. 1c. Fluorescence

spectra of phOx-fluorescein bound to sFv and of unbound phOx-fluorescein in solution had similar spectral shapes (Fig. 1c). As intended, the fluorescence of the unbound conjugate was decreased considerably (by 5-fold) over that of the bound conjugate. Images of CHO cells expressing sFv at the plasma membrane were acquired with increasing concentration of phOx-fluorescein. The fluorescence from sFv-bound phOx-fluorescein gave a dissociation constant ( $K_d$ ) of 6.8 nM (Fig. 1d). This agrees with the value of 5.5 nM obtained in CHO cell suspensions expressing sFv at the plasma membrane (not shown). At 10 nM phOx-fluorescein, fluorescence from free dye was 75 times lower than that of bound dye. No significant fluorescence from non-sFv-expressing cells was seen.

The toxicity and stability of the conjugates were investigated. There were no differences in cell growth as assessed by cell counting and viability as assessed by trypan blue exclusion between control cells and cells incubated for 24 h with 200 nM of each conjugate. The stability of the imine bond in the conjugates was determined in cells. In freshly prepared phOx-fluorescein and phOx-fluorescein incubated with cell suspensions for up to 7 h, the imine bond was hydrolyzed in 0.5 M NaOH, resulting in increased fluorescence. The fluorescence increase after treatment with NaOH was the same in both samples, indicating that the imine bond was not hydrolyzed in cells.

The various sFv targeting constructs and phOx conjugates were studied in CHO cells. Fig. 2a shows a fluorescence image of living cells expressing the sFv at the plasma membrane and labeled with phOx-rhodamine. A plasma membrane staining pattern was found. Fig. 2b shows staining of sFv in the same cells with a fluorescein-labeled anti-c-Myc antibody. Comparison with Fig. 2a demonstrates that only sites of sFv expression

were significantly labeled with phOx-rhodamine. There was no significant staining of adjacent cells that did not express sFv (Fig. 2c). Fig. 2d shows specific phOx-Bodipy staining of Golgi. Staining was reversed by addition of 1  $\mu$ M phOx-ethanolamine (Fig. 2e) but not by 1  $\mu$ M ethanolamine. Fig. 2f shows phOx-Bodipy staining of ER, seen as a characteristic reticular pattern. The high expression level of the sFv, the relatively high affinity of the hapten/sFv, and the low fluorescence of the

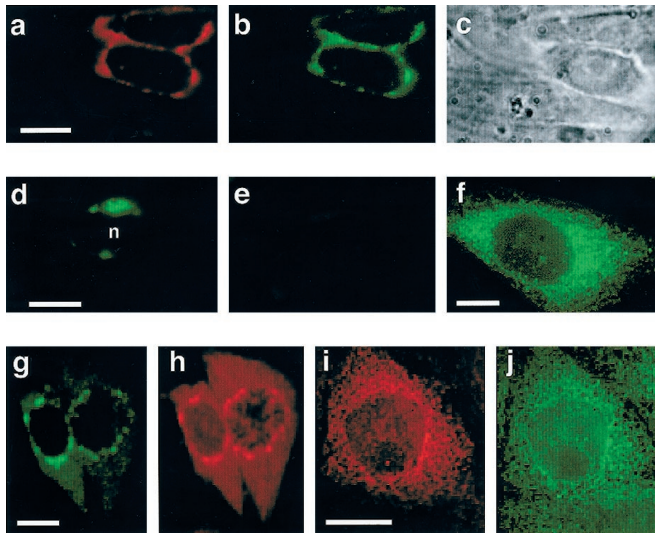
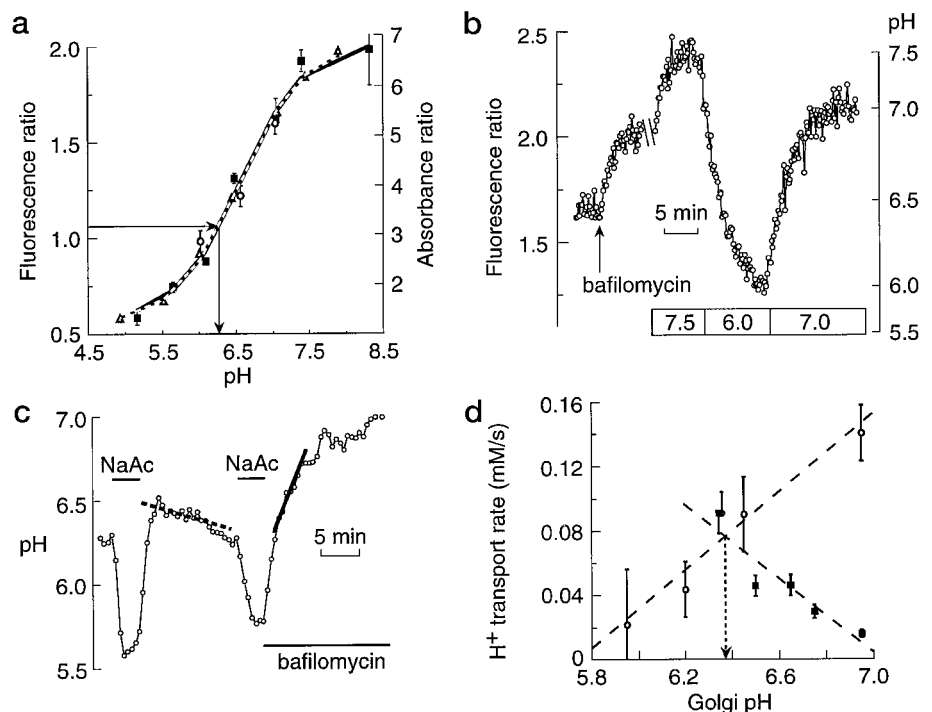


**FIG. 2. Site-specific labeling of CHO cells.** *a*, confocal fluorescence image of CHO cells transfected with the plasma membrane-targeted sFv vector and stained with phOx-rhodamine. *b*, confocal fluorescence image of cells stained with a fluorescein-labeled anti-c-Myc antibody. *c*, bright field image of cells in *a*. *d*, fluorescence image of CHO cells with Golgi-targeted sFv in the presence of 10 nM phOx-Bodipy FL (*n*, nucleus). *e*, same cells as in *d* in the presence of 1  $\mu$ M phOx-ethanolamine and 10 nM phOx-Bodipy FL. *f*, fluorescence image of cell with ER-targeted sFv in the presence of 10 nM phOx-Bodipy FL. Immunostaining of Golgi-sFv-transfected cells with fluorescein-labeled, anti-c-Myc antibody (*g*) and rhodamine-labeled anti-mouse antibody directed against a mouse 58-kDa protein antibody (*h*) is shown. Immunostaining of ER-sFv-transfected cells with rhodamine-labeled anti-mouse antibody directed against an anti-c-Myc antibody (*i*) and fluorescein-labeled concanavalin A (*j*) is shown. Scale bars, 10  $\mu$ m.

**FIG. 3. Measurement of Golgi pH.** *a*, average ratio generated by pixel-by-pixel division of 490-nm images by 440-nm images after background subtraction was converted to pH using a calibration relating pH to fluorescence signal ratios for Golgi (circles) and plasma membrane (squares) targeted phOx-fluorescein. Plasma membrane data were acquired in the presence of 10 nM phOx-fluorescein. The ratios of absorbance at 490-to-440 nm are shown for unbound phOx-fluorescein (triangles) in solution. Calibration data were fitted to a single site titration model (solid line, fluorescence; dashed line, absorbance). *b*, fluorescence ratio (490/440) time course in Golgi. At indicated times, bafilomycin A<sub>1</sub> (100 nM) and high K<sup>+</sup> buffers (120 mM) containing 5  $\mu$ M monensin at indicated pH were added. Calibration solutions were used to convert ratios to pH values (scale at right). *c*, calculated pH time course in response to a 20 mM sodium acetate prepulse in the absence and presence of 100 nM bafilomycin A<sub>1</sub>. Lines (fitted from 120 to 300 s after prepulse) indicate the initial rate of pH change. *d*, calculated proton pump rates (circles) and leak rates (filled squares) as a function of Golgi pH are shown. Dashed lines are linear fits to the data.



unbound conjugate allowed images to be obtained in the presence of <10 nM of unbound conjugate with little contribution from free conjugate. Leakage out of the Golgi, which required dissociation from the sFv and diffusion through lipid membranes and unstirred layers, had a half-time of tens of minutes.

The subcellular location of expressed sFv was confirmed by immunofluorescence. Cells transfected with the Golgi-sFv construct showed perinuclear staining by a fluorescein-labeled, anti-c-Myc antibody (Fig. 2g), which colocalized with staining by antibodies against the Golgi marker 58-kDa protein (14) (Fig. 2h). Cells transfected with the ER-sFv construct showed a reticular staining pattern with the c-Myc antibody (Fig. 2i), which colocalized with staining by fluorescein-labeled concanavalin A, an ER marker (15) (Fig. 2j). The membrane permeability of the conjugates was high enough to load cells by incubation at 37 °C for 4 h for phOx-fluorescein, 2 h for phOx-rhodamine, or 10 min for the less polar phOx-Bodipy. Cells could be loaded at 4 °C, indicating that the conjugate entered the cells primarily by transmembrane diffusion and not by endocytosis. These results demonstrate the selective targeting of fluorescent probes to expressed sFv in living cells.

Organelle-specific sFv targeting was applied to measure Golgi pH using phOx-fluorescein as the probe. Ratio images were calculated from images of Golgi labeled with phOx-fluorescein acquired at 440- and 490-nm excitation wavelengths. To convert ratios to absolute pH, cells were perfused with "calibration buffers" at different pH values containing high K<sup>+</sup> and the ionophore monensin to equalize extracellular and Golgi luminal pH. The dependence of the fluorescence ratio on pH was measured for Golgi and plasma membrane-expressed sFv (Fig. 3a). The apparent  $pK_a$  of 6.56 of bound phOx-fluorescein was not different from that of unbound phOx-fluorescein in solution ( $pK_a$  = 6.54). The average Golgi fluorescence ratio of  $1.05 \pm 0.05$  corresponds to a pH of  $6.25 \pm 0.06$ , in agreement with previous estimates (7, 16, 17).

The Golgi-targeted phOx-fluorescein was used to detect continuous changes in luminal pH in individual cells. Fig. 3b shows that the fluorescence ratio increases upon addition of the vacuolar H<sup>+</sup> pump inhibitor bafilomycin A<sub>1</sub>. The ratios measured using calibration buffers were used to convert fluores-



cence ratios to pH (scale at right). Golgi pH initially at  $\sim 6.3$  promptly alkalized after the addition of bafilomycin  $A_1$ .

It has been proposed that the steady-state Golgi pH is determined thermodynamically by the free energy of ATP hydrolysis used by the vacuolar  $H^+$ /ATPase to pump  $H^+$  against an electrochemical gradient (13). To test the model prediction that the  $H^+$  pump rate is 0 at steady-state pH, the rates of Golgi  $H^+$  pump and leak were measured as a function of Golgi luminal pH. After Golgi alkalization by a 20 mM sodium acetate prepulse,  $H^+$  pumping into the Golgi restores steady-state pH (Fig. 3c). The initial rate of pH change (dashed line) is the difference between pump and leak rates:  $dpH/dt = (dH^+/dt_{\text{leak}} - dH^+/dt_{\text{pump}})/\beta$ . The buffer capacity,  $\beta$ , was measured by the  $NH_4Cl$  pulse method (18) to be constant ( $38 \pm 3$  mM/pH units) in the pH range 6–7 (not shown). The  $H^+$  leak rate,  $dH^+/dt_{\text{leak}}$ , was measured from the pH change (Fig. 3c, solid line) after an identical 20 mM sodium acetate prepulse with the  $H^+$  pump inhibited by bafilomycin  $A_1$ . Similar prepulse measurements were done at different Golgi pH by varying sodium acetate and  $NH_4Cl$  concentrations. There should be little effect of acetate or  $NH_4^+$  on  $H^+$  transport in the prepulse method because these ions have left the cell by the time of the  $H^+$  transport measurements (18). Fig. 3d shows that the computed  $H^+$  pump rate increases sharply with Golgi pH and that the pump rate is not 0 at the Golgi steady-state pH of  $\sim 6.25$ . Although it is recognized that the prepulse method used to alter Golgi pH also alters cytoplasmic pH, it has been reported that the  $H^+$  pump rate is relatively insensitive to cytoplasmic pH in both mammalian (17) and plant (19) systems.

In the steady state,  $H^+$  pump rate must equal  $H^+$  leak rate. The dependence of the leak rate on Golgi pH was measured from the kinetics of pH change after bafilomycin  $A_1$  addition as shown in Fig. 3b. The data for different pH are summarized in Fig. 3d, showing decreased  $H^+$  leak as Golgi pH increases. The intersection of the  $H^+$  pump and leak curves predicts correctly the observed steady-state Golgi pH, supporting a balanced pump/leak mechanism for setting Golgi pH.

#### DISCUSSION

The fluorophore targeting method reported here provides a new strategy for cellular labeling that complements existing methods. Of the current methods, GFP is the easiest to use because it does not require exogenously added reagents or cofactors. However, the available GFP mutants are limited in terms of spectral properties (brightness and excitation and emission wavelengths) and indicator sensitivities. Recently, a method was developed for covalently labeling proteins in living cells with a fluorescein derivative (FLASH) (20). Addition of an arseno-fluorescein derivative to the cells leads to covalent attachment of the derivative to a short  $\alpha$ -helix containing 4 cysteines added to the protein of interest. An advantage of FLASH over GFP and the current approach is the significantly smaller size of the protein tag; however, FLASH is currently limited to the use of fluorescein as the probe.

The addition of labeled macromolecules either requires microinjection (21) or is limited to compartments that are accessible by endocytosis (22) or retrograde transport through the secretory pathway (17). GFP, FLASH, and the receptor-mediated targeting methods use genetically encoded targeting sequences to localize fluorophores to virtually any cellular site, provided that the targeted protein is able to fold properly. Although strong sFv expression was found in plasma membranes and various intracellular compartments (Fig. 2, above), preliminary experiments suggest that functional sFv expression is relatively poor in reducing environments (data not shown). If disulfide bond formation is critical to sFv folding, it may be possible to generate sFv mutants lacking disulfide

bonds that fold well in reducing environments (23).

The ability to target fluorophores of varied spectral properties is a distinct advantage of the receptor-mediated targeting approach over GFP. The receptor-mediated targeting method utilizes fluorescent probes with a potentially wide range of excitation and emission wavelengths and other optical properties. The use of multiple probes with well separated excitation and emission spectra allows simultaneous labeling of multiple sites. For measurements of important cellular parameters, small chemical probes sensitive to ions ( $Ca^{2+}$ ,  $Na^+$ ,  $K^+$ ,  $H^+$ ,  $Cl^-$ ), viscosity, and membrane potential are available.

Receptor-mediated targeting of a hapten-fluorescein conjugate was used to label the Golgi with a fluorescent pH indicator permitting the measurement of the dependence of the vacuolar  $H^+$ /ATPase pump rate on Golgi pH. The pump rate increased and the leak rate decreased as Golgi pH increased. The steep dependence of pump rate on pH is in agreement with measurements of ATPase activity (24) of the vacuolar  $H^+$ /ATPase made *in vitro* and of the pump rate made in phagosomes (25). In contrast to the predictions of a thermodynamic model of pH regulation in the Golgi, the net pump rate was not 0 at the resting Golgi pH. Thus, the resting pH is determined by the kinetics of proton leak *versus* pump. Shifts in the leak or pump curves could account for the differences in resting pH in organelles of the secretory pathway.

In summary, the receptor-mediated probe targeting strategy allows the labeling of specified cellular structures with fluorescent or other indicator molecules. This targeting method can readily be extended to deliver conjugates containing magnetic resonance probes, caged compounds, or chemical cross-linkers. Finally, the use of cell-specific promoters and gene transfer should allow the *in vivo* targeting of hapten-probe complexes to specific cell types in multicellular organisms.

**Acknowledgments**—We thank Dr. J. Biwersi for help with organic synthesis and Drs. T. Ma and Y. Li for help in vector construction.

#### REFERENCES

1. Tsien, R. Y. (1992) *Am. J. Physiol.* **263**, C723–C728
2. Seksek, O., Biwersi, J., and Verkman, A. S. (1997) *J. Cell Biol.* **138**, 131–142
3. Chalfie, M., Tu, Y., Euskirchen, G., Ward, W. W., and Prasher, D. C. (1994) *Science* **263**, 802–804
4. Cubitt, A. B., Heim, R., Adams, S. R., Boyd, A. E., Gross, L. A., and Tsien, R. Y. (1995) *Trends Biochem. Sci.* **20**, 448–455
5. Orm6, M., Cubitt, A. B., Kallio, K., Gross, L. A., Tsien, R. Y., and Remington, S. J. (1996) *Science* **273**, 1392–1395
6. Kneen, M., Farinas, J., Li, Y., and Verkman, A. S. (1998) *Biophys. J.* **74**, 1591–1600
7. Llopis, J., McCaffery, J. M., Miyawaki, A., Farquhar, M. G., and Tsien, R. Y. (1998) *Proc. Natl. Acad. Sci. U. S. A.* **95**, 6803–6808
8. Miesenböck, G., De Angelis, D. A., and Rothman, J. E. (1998) *Nature* **394**, 192–195
9. Miyawaki, A., Llopis, J., Heim, R., McCaffery, J. M., Adams, J. A., Ikura, M., and Tsien, R. Y. (1997) *Nature* **388**, 882–887
10. Rosomov, V. A., Hinkle, P. M., and Persechini, A. (1997) *J. Biol. Chem.* **272**, 13270–13274
11. Siegel, M. S., and Isacoff, E. Y. (1997) *Neuron* **19**, 735–741
12. Chestnut, J. D., Baytan, A. R., Russell, M., Chang, M., Bernard, A., Maxwell, I. H., and Hoeffler, J. (1996) *J. Immunol. Methods* **193**, 17–27
13. Rybak, S. L., Lanni, F., and Murphy, R. F. (1997) *Biophys. J.* **73**, 674–687
14. Bloom, G. S., and Brashear, T. A. (1989) *J. Biol. Chem.* **264**, 16083–16092
15. Virtanen, I., Ekblom, P., and Laurila, P. (1980) *J. Cell Biol.* **85**, 429–434
16. Seksek, O., Biwersi, J., and Verkman, A. S. (1995) *J. Biol. Chem.* **270**, 4967–4970
17. Kim, J. H., Lingwood, C. A., Williams, D. B., Furuya, W., Manolson, M. F., and Grinstein, S. (1996) *J. Cell Biol.* **134**, 1387–1399
18. Roos, A., and Boron, W. F. (1981) *Physiol. Rev.* **61**, 296–421
19. Davies, J. M., Hunt, I., and Sanders, D. (1994) *Proc. Natl. Acad. Sci. U. S. A.* **91**, 8547–8551
20. Griffin, B. A., Adams, S. R., and Tsien, R. Y. (1998) *Science* **281**, 269–272
21. Swedlow, J. R., Sedat, J. W., and Agard, D. A. (1993) *Cell* **73**, 97–108
22. Demareux, N., Furuya, W., D'Souza, S., Bonifacio, J. S., and Grinstein, S. (1998) *J. Biol. Chem.* **273**, 2044–2051
23. Proba, K., W6rn, A., Honegger, A., and Pl6ckthun, A. (1998) *J. Mol. Biol.* **275**, 245–253
24. Arai, K., Shimaya, A., Hiratani, N., and Ohkuma, S. (1993) *J. Biol. Chem.* **268**, 5649–5660
25. Lukacs, G. L., Rotstein, O. D., and Grinstein, S. (1991) *J. Biol. Chem.* **266**, 24540–24548

## Receptor-mediated Targeting of Fluorescent Probes in Living Cells

Javier Farinas and A. S. Verkman

*J. Biol. Chem.* 1999, 274:7603-7606.

doi: 10.1074/jbc.274.12.7603

---

Access the most updated version of this article at <http://www.jbc.org/content/274/12/7603>

### Alerts:

- [When this article is cited](#)
- [When a correction for this article is posted](#)

[Click here](#) to choose from all of JBC's e-mail alerts

This article cites 25 references, 14 of which can be accessed free at <http://www.jbc.org/content/274/12/7603.full.html#ref-list-1>